Numerical Integration of Primitive Equations by a Quasi-Lagrangian Advective Scheme

T. N. KRISHNAMURTI

University of California, Los Angeles, Calif.

(Manuscript received 21 June 1962)

ABSTRACT

A quasi-Lagrangian advective scheme for numerical integration of primitive equations is proposed. The advective scheme is built on a successive approximation procedure where the Fjørtoft-type of quasi-Lagrangian advection forms an initial guess. The numerical program is tested by constructing some simple analytic problems containing the non-linear advective terms. It is shown that the scheme is also capable of producing very reasonable numerical forecasts for simple initial conditions for problems of mixed and filtered wave motions.

1. Introduction

The simple quasi-Lagrangian advection scheme is familiar to meteorologists through the graphical forecast models and several numerical forecast models. The principal forecast equations are the quasi-geostrophic vorticity equations where the non-meteorological gravity-inertia modes are absent.

Fjørtoft (1952, 1955) introduced the working scheme for a barotropic and simple baroclinic model where one traces air parcels by virtue of their conservative properties such as the absolute and potential vorticities. The numerical forecast models proposed by Sawyer,[1] Wiin-Nielsen (1959) and Økland (1962) are similar schemes for tracking air parcels for short time periods on a high speed computer. The conservative properties of the parcel are advected along a smoothed steamfunction field and forecast fields are obtained by a simple relaxation procedure. The recent work of Charney,[2] on numerical weather prediction as an N-vortex problem, is essentially a quasi-Lagrangian scheme where one keeps track of the potential vorticity of the flow as the conservative property.

The author wishes to propose through this paper a quasi-Lagrangian advection scheme which is a generalization of Fjørtoft's scheme (1952). The scheme will be illustrated for application to the undifferentiated primitive form of the equations of motion. The conventional quasi-Lagrangian advection schemes based on the quasi-geostrophic theory and the one to be presented here differ primarily in that the advection will be carried out for non-conservative fields where we shall not look for any special properties of an air parcel. Because of the non-conservative nature of the field we shall utilize very small time steps and allow for the variation of the field during the integration time steps.

We propose to build the advection scheme by a successive approximation method where the simple Fjørtoft type of advection will form the first or a second guess. We shall select a class of non-linear hydrodynamical problems containing the advective terms and compare the exact analytic solutions with the numerical solutions obtained.

2. The proposed advection scheme

Three main phases constitute the advection scheme:

(i) A guess on the coordinate of the parcel.

(ii) An efficient time integration scheme during each guess. This scheme is built by methods very similar to those of Runge Kutta and Euler, illustrated in several text books on numerical integration of differential equations (e.g., Levy and Baggott, 1950).

(iii) An objective analysis phase. This could be one of a local nature or one that covers an entire grid over a large area.

In the actual integration of meteorological (primitive) equations one would need to consider the computational stability criteria of any finite difference scheme. We shall discuss this aspect later in this paper when we consider the actual integration of a meteorological problem. Now we shall assume that the computational stability criteria are satisfied for the proposed advection scheme by a proper choice of a grid spacing.

[1] Sawyer, J. S., 1960: Experiments in integrating the vorticity advection equation by a Lagrangian method. Technical Note (B) Meteorological Office, Dunstable, England.

[2] Charney, J., 1962: Numerical weather prediction in three dimensions as an N-vortex problem. Paper presented at the Fourth Numerical Weather Prediction Conference at Los Angeles, Calif., January 1962.

Consider the following system of equations describing the flow of a fluid in a two-dimensional plane

$$\frac{du}{dt}=\frac{\partial u}{\partial t}+u\frac{\partial u}{\partial x}+v\frac{\partial u}{\partial y}=P \tag{1}$$

$$\frac{dv}{dt}=\frac{\partial v}{\partial t}+u\frac{\partial v}{\partial x}+v\frac{\partial v}{\partial y}=Q \tag{2}$$

$$\frac{dz}{dt}=\frac{\partial z}{\partial t}+u\frac{\partial z}{\partial x}+v\frac{\partial z}{\partial y}=R \tag{3}$$

$$\frac{dA}{dt}=\frac{\partial A}{\partial t}+u\frac{\partial A}{\partial x}+v\frac{\partial A}{\partial y}=S \tag{4}$$

$$\frac{dB}{dt}=\frac{\partial B}{\partial t}+u\frac{\partial B}{\partial x}+v\frac{\partial B}{\partial y}=T. \tag{5}$$

u and v are the two velocity components along the x and y axes. z, A and B are other dependent variables of the problem, P, Q, R, S, and T are functions of the coordinates x, y and t and the variables u, v, z, A and B. (These may be linear or non-linear functions.)

The numerical aspects of advection. The following notation will be used to describe a quantity Q

$$Q\equiv Q_{ij}^{np} \quad \begin{matrix}\text{time step}\\ \text{x-coordinate}\end{matrix} \quad \begin{matrix}\text{guess number}\\ \text{y-coordinate}\end{matrix}.$$

At time $t=0$ we shall assume the following quantities to be given on a grid network: u_{ij}^{00}, v_{ij}^{00}, z_{ij}^{00}, A_{ij}^{00}, B_{ij}^{00}. We shall assume that the quantities P_{ij}^{00}, Q_{ij}^{00}, R_{ij}^{00}, S_{ij}^{00} and T_{ij}^{00} are then evaluated at the grid points according to their functional forms. The meaning of the quantity p, the guess, will become clear in the following analysis.

(i) *Guess zero.* During each time step n, the program is initiated by the guess zero. The question asked is where did a parcel, now at coordinate $i=I$, $j=J$ originate. We set, for $n=1$,

$$(\Delta x)_{ij}^{10}=0 \tag{6}$$

$$(\Delta y)_{ij}^{10}=0 \tag{7}$$

Eq (6) and (7) describe the distances along the x and y axes from the grid point I, J.

When the origin of a parcel is known, a time integration is carried out by a first-forward then-centered implicit scheme, the later being repeated many times for high accuracy. This time integration along the trajectory of the parcel is a generalization of the Runge-Kutta type of scheme for numerical integration of many simultaneous ordinary differential equations. It will be shown that the time truncation errors can be made very small by this procedure.

The equations describing the first forward difference over a time step Δt, may be written as

$$u_{ij}^{10}=u_{ij}^{00}+P_{ij}^{00}\Delta t \tag{8}$$

$$v_{ij}^{10}=v_{ij}^{00}+Q_{ij}^{00}\Delta t \tag{9}$$

$$z_{ij}^{10}=z_{ij}^{00}+R_{ij}^{00}\Delta t \tag{10}$$

$$A_{ij}^{10}=A_{ij}^{00}+S_{ij}^{00}\Delta t \tag{11}$$

$$B_{ij}^{10}=B_{ij}^{00}+T_{ij}^{00}\Delta t. \tag{12}$$

The corresponding magnitudes of P_{ij}^{10}, Q_{ij}^{10}, R_{ij}^{10}, S_{ij}^{10}, T_{ij}^{10} may then be evaluated from the computed quantities given by Eq (8) to (12).

The centered implicit time difference scheme is now introduced by the following set of equations

$$u_{ij}^{10}=u_{ij}^{00}+\tfrac{1}{2}(P_{ij}^{00}+P_{ij}^{10})\Delta t \tag{13}$$

$$v_{ij}^{10}=v_{ij}^{00}+\tfrac{1}{2}(Q_{ij}^{00}+Q_{ij}^{10})\Delta t \tag{14}$$

$$z_{ij}^{10}=z_{ij}^{00}+\tfrac{1}{2}(R_{ij}^{00}+R_{ij}^{10})\Delta t \tag{15}$$

$$A_{ij}^{10}=A_{ij}^{00}+\tfrac{1}{2}(S_{ij}^{00}+S_{ij}^{10})\Delta t \tag{16}$$

$$B_{ij}^{10}=B_{ij}^{00}+\tfrac{1}{2}(T_{ij}^{00}+T_{ij}^{10})\Delta t. \tag{17}$$

The quantities P_{ij}^{10}, Q_{ij}^{10}, R_{ij}^{10}, S_{ij}^{10}, T_{ij}^{10} are then recomputed and this centered implicit scheme is repeated until the difference between the new value of $|Q_{ij}^{10}|$ and the one-previous value of $|Q_{ij}^{10}|$ are less than a certain small magnitude ϵ.

(ii) *Guess one.* The new origin of the parcel is determined by the following pair of equations:

$$(\Delta x)_{ij}^{11}=\tfrac{1}{2}(u_{ij}^{00}+u_{ij}^{10})\Delta t \tag{18}$$

$$(\Delta y)_{ij}^{11}=\tfrac{1}{2}(v_{ij}^{00}+v_{ij}^{10})\Delta t. \tag{19}$$

The objective analysis phase is introduced at this stage. In this paper we shall use a nine-point local objective analysis technique shown in Fig. 1. A quantity Q_{ij}^{10} will

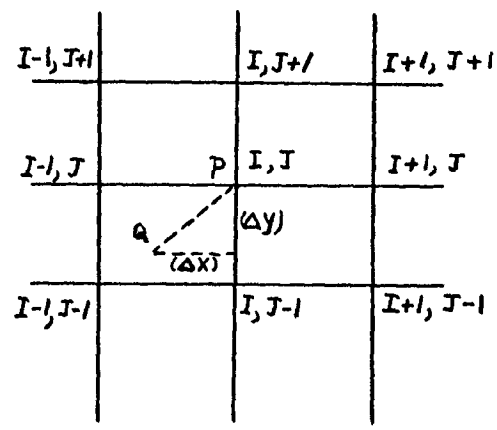

FIG. 1. The nine points of the objective analysis phase for each grid point $P(I,J)$. The origin of the parcel is given by a point Q.

be expanded by the series

$$Q_{ij}^{10}=\sum_{N=0}^{2}\sum_{M=0}^{2}\eta_{MN}x^{M}y^{N}. \tag{20}$$

The nine coefficients η_{MN} may be determined from the data at the nine points of Fig. 1. The obvious purpose of the objective analysis is to determine the magnitude of Q_{ij}^{01} when the origin is not one of the nine points but lies inside one of the rectangles. The objective analysis scheme given by Eq (20) is one of many possible schemes. It can be shown that the space truncation errors can be reduced considerably by a scheme containing many expansion coefficients of this type or better still one containing coefficients of many wave numbers in a double-Fourier series type of expansion. Some numerical experiments are being carried out to formulate this problem for higher order coefficient representation.

Eq (18), (19) and (20) enable us to obtain the quantities u_{ij}^{01}, v_{ij}^{01}, z_{ij}^{01}, A_{ij}^{01}, B_{ij}^{01}, the variables at the origin, for the first guess. Corresponding values of P_{ij}^{01}, Q_{ij}^{01}, R_{ij}^{01}, S_{ij}^{01} and T_{ij}^{01} may be obtained from their functional dependence. The time iteration procedure of guess zero is repeated at this stage (first forward, then centered implicit iterative).

(iii) *Guesses, $p>1$.* Then the program proceeds to $p>1$ and the calculations are carried out in the same manner as for $p=1$. The calculations are repeated until

$$(|Q_{ij}^{1p}|-|Q_{ij}^{1p-1}|)<\epsilon. \tag{21}$$

The convergence suggested by Eq (21) is not demonstrated by an analytic proof. The author has carried out a very wide range of numerical experiments to test the program proposed above and has found that the scheme does converge. The class of problems tested will be presented in this paper.

We may summarize the main aspects of the numerical program as follows. The integrations are carried out along very short trajectories, along which we do not necessarily assume conservation of any property. No non-linear advective terms appear in this formulation of the problem. The successive approximation scheme enables us to answer in particular the question, "Where did a parcel now at a grid point I, J originate?" Once the origin is determined we integrate along the trajectory to determine forecasts for the point I, J. This procedure is continued.

3. Class of simple non-linear problems with exact analytic solutions

In this section we wish to introduce a class of problems describing the flow of a fluid on a two dimensional plane for certain simple initial conditions.

Consider the system of equations for the two unknowns u and v,

$$\frac{du}{dt}=\frac{\partial u}{\partial t}+u\frac{\partial u}{\partial x}+v\frac{\partial u}{\partial y}=P$$

$$\frac{dv}{dt}=\frac{\partial v}{\partial t}+u\frac{\partial v}{\partial x}+v\frac{\partial v}{\partial y}=Q.$$

On an infinite plane along the coordinates x and y let,

$$u(x,y,0)=Ax+By \tag{22}$$

$$v(x,y,0)=Cx-Ay \tag{23}$$

where A, B and C are arbitrary constants. These initial conditions are selected because of their simplicity and for the reason that it is possible to obtain analytic solution for various functions P and Q. The streamlines of the initial field are given by the non-linear differential equation

$$(Ax+By)\frac{dy}{dx}=(Cx-Ay). \tag{24}$$

The streamlines described by Eq (24) display a variety of flow patterns for different magnitudes of A, B and C. Some such flow patterns have been discussed by Van-Mieghem (1951). We shall now write down the solutions for the initial value problem proposed here, for various functions P and Q.

---

a) $P=Q=0$

$$\begin{matrix}u\\v\end{matrix}=\frac{\begin{matrix}A\\C\end{matrix}\left\{(1-At)x-Bty\right\}\pm\begin{matrix}B\\A\end{matrix}\left\{(1+At)y-Ctx\right\}}{1-(A^2+BC)t^2} \tag{25}$$

b) $P=g$, $Q=h$ P and Q are constants.

$$\begin{matrix}u\\v\end{matrix}=\frac{\begin{matrix}A\\C\end{matrix}\left\{(1-At)\left(x-\frac{gt^2}{2}\right)-Bt\left(y-\frac{ht^2}{2}\right)\right\}\pm\begin{matrix}B\\A\end{matrix}\left\{(1+At)\left(y-\frac{ht^2}{2}\right)-Ct\left(x-\frac{gt^2}{2}\right)\right\}}{1-(A^2+BC)t^2} \tag{26}$$

c) $P=\alpha u$, $Q=\alpha v$ where α is a constant.

$$\frac{u}{v}=\frac{\pm e^{\alpha t}\left[\begin{matrix}x\\y\end{matrix}\left(A\mp\frac{1}{\alpha}(A^2+BC)(e^{\alpha t}-1)\pm\begin{matrix}yB\\xC\end{matrix}\right)\right]}{1-\frac{1}{\alpha^2}(A^2+BC)(e^{\alpha t}-1)^2} \tag{27}$$

d) $P=fv$, $Q=-fu$, where f is a constant (a mean value of the coriolis parameter). The solutions describe pure inertial oscillations.

Let

$$l_1=\frac{B\cos ft}{f}-\frac{A\sin ft}{f}-\frac{B}{f}+1$$

$$l_2=\frac{B\sin ft}{f}+\frac{A\cos ft}{f}-\frac{A}{f}$$

$$l_3=\frac{A\sin ft}{f}-\frac{C\cos ft}{f}+\frac{c}{f}+1$$

and

$$l_4=\frac{C\sin ft}{f}+\frac{A\cos ft}{f}-\frac{A}{f}$$

then

$$\frac{u}{v}=\frac{\left[\left\{\begin{matrix}A\\C\end{matrix}(l_1x-l_2y)\pm\begin{matrix}B\\A\end{matrix}(l_3y-l_4x)\right\}\cos ft\pm\left\{\begin{matrix}C\\A\end{matrix}(l_1x-l_2y)\pm\begin{matrix}A\\B\end{matrix}(l_3y-l_4x)\right\}\sin ft\right]}{(l_1l_3-l_2l_4)}. \tag{28}$$

The solutions given above are obtained by a Lagrangian integration scheme called the Jean's theorem. This method has found application in some simple problems in magneto-hydrodynamics. We shall illustrate one example in Appendix I. The infinite-plane solutions given above are obtained by this method.

We shall next demonstrate some tests of the numerical program for the problems listed above.

(a) *The grid spacing and the initial and boundary conditions*

A rectangular area of dimension 1000 km square, with a grid spacing $\Delta x=\Delta y=100$ km is selected. The following constants define the initial distribution of Eq (22) and (23):

$$A=10^{-5},\quad B=10^{-5},\quad \text{and}\quad C=4\times10^{-5}.$$

The boundary conditions are prescribed by the exact solutions along the four corner lines, such that the dynamical properties of the parcels are given for all time.

(b) *Results of the numerical calculations*

Tables 1, 2 and 3 show the first time step integration at two arbitrary grid points for the first three examples. The computed values of u_{ij}^{1p}, v_{ij}^{1p}, $(\Delta x)_{ij}^{1p}$ and $(\Delta y)_{ij}^{1p}$ are shown for different guesses. The analytic solution is given at the bottom row. In the three cases the time steps Δt were, respectively, 1 hr, 1 hr and $\frac{1}{4}$ hr. Of particular interest is the rate of convergence for given ϵ, which is determined by the largest magnitude of p. A very small number of guesses $p<10$ were required to carry out the convergence for $\epsilon\leq10^{-6}$. For a larger ϵ the rate of convergence was found to be faster.

Table 4 shows the results of a 12-hr integration for the inertial motions. A time step $\Delta t=1$ min was used in these calculations. The analytic solution has been reproduced to 6 figures by two objective analysis schemes (i) a nine point scheme and (ii) a five point scheme. The latter is determined from an equation of the type

$$Q=ax^2+by^2+cx+dy+e. \tag{29}$$

The five coefficients a, b, c, d and e are determined by the five points (four points surrounding a grid point in the conventional sense). We have also included in this table the results of the calculation at the same grid point by a simple Eulerian integration scheme. The Eulerian scheme was constructed by a simple first forward then centered difference in time, all space derivatives were centered, and the boundary conditions were the same as in the quasi-Lagrangian representation.

TABLE 1. The numerical integration of the first time step for $\frac{du}{dt}=\frac{dv}{dt}=0$ at two arbitrary grid points.

(Units: meters per second. Time step $\Delta t=1$ hr.)

Initial value	u 1.000000	v 4.000001	Δx	Δy	Initial value	u 16.000005	v 24.000007	Δx	Δy
Forecast					Forecast				
Guess number					Guess number				
0	1.000000	4.000001	0	0	0	16.000005	24.000007	0	0
1	.820000	4.000001	3600.001	14400.00	1	14.560004	22.560006	57600.01	86400.02
2	.826480	4.025921	2952.000	14400.00	2	14.663684	22.715526	52416.01	81216.02
3	.825314	4.025921	2975.328	14493.31	3	14.654353	22.706195	52789.26	81775.89
4	.825356	4.026089	2971.129	14493.31	4	14.655025	22.707203	52755.66	81742.30
5	.825348	4.026089	2971.280	14493.92	5	14.654964	22.707142	52758.08	81745.92
6	.825349	4.026090	2971.253	14493.92	6	14.654969	22.707149	52757.87	81745.71
7	.825348	4.026090	2971.254	14493.92	7	14.654968	22.707149	52757.88	81745.73
8					8	14.654968	22.707148	52757.88	81745.73
9					9				
Exact solution	.825348	4.026090			Exact solution	14.654968	22.707148		

TABLE 2. The numerical integration of the first time step for $\frac{du}{dt}=g$, $\frac{dv}{dt}=h$ at two arbitrary grid points.

(Units: meters per second. Time step $\Delta t=1$ hr.)

Initial value	u 2.000001	v 8.000002	Δx	Δy	Initial value	u 15.000004	v 20.000006	Δx	Δy
Forecast					Forecast				
Guess number					Guess number				
0	3.000001	9.000002	0	0	0	16.000004	21.000006	0	0
1	2.604000	8.946002	9000.001	30600.00	1	14.704004	19.506005	55800.01	73800.02
2	2.620200	9.001082	7574.401	30405.60	2	14.804444	19.638845	51134.41	68421.61
3	2.617634	9.000732	7632.721	30603.89	3	14.796046	19.629164	51495.99	68899.84
4	2.617739	9.001089	7623.483	30602.63	4	14.796696	19.630025	51465.76	68864.98
5	2.617723	9.001087	7623.861	30603.92	5	14.796642	19.629962	51468.10	68868.08
6	2.617723	9.001089	7623.801	30603.91	6	14.796646	19.629967	51467.91	68867.86
7					7				
8					8				
9					9				
Exact solution	2.617723	9.001089			Exact solution	14.796646	19.629967		

TABLE 3. The numerical integration of the first time step for $\frac{du}{dt}=\alpha u$, $\frac{dv}{dt}=\alpha v$ at two arbitrary grid points.

(Units: meters per second. Time step $\Delta t=\frac{1}{4}$ hr.)

Initial value	u 1.000000	v 4.000001	Δx	Δy	Initial value	u 3.000001	v 12.000004	Δx	Δy
Forecast					Forecast				
Guess number					Guess number				
0	1.051282	4.205129	0	0	0	3.153847	12.615388	0	0
1	1.002762	4.205129	923.0771	3692.308	1	3.008285	12.615388	2769.231	11076.92
2	1.003210	4.206921	880.4736	3692.308	2	3.009629	12.620763	2641.420	11076.92
3	1.003189	4.206921	880.8668	3693.881	3	3.009566	12.620763	2642.600	11081.64
4	1.003189	4.206922	880.8487	3693.881	4	3.009567	12.620765	2642.546	11081.64
5					5				
6					6				
7					7				
8					8				
9					9				
Exact solution	1.003189	4.206922			Exact solution	3.009566	12.620765		

TABLE 4. The numerical integration for the pure inertial motions $\frac{du}{dt}=fv$, $\frac{dv}{dt}=-fu$ at an arbitrary grid point.

(Units: meters. Time step $\Delta t=60$ sec. The numbers show the forecast values for u.)

Time (hr)	Analytic solution	An Eulerian scheme	Quasi-Lagrangian scheme 5-Point	Quasi-Lagrangian scheme 9-Point
1	4.120922	4.086989	4.120919	4.120191
2	1.938031	1.898766	1.938026	1.938026
3	−0.618639	−0.665189	−0.618633	−0.618633
4	−3.678585	−3.734694	−3.678580	−3.678580
5	−7.354246	−7.420924	−7.354242	−7.354242
6	−11.525134	−11.595576	−11.525129	−11.525129
7	−15.110157	−15.150965	−15.110150	−15.110150
8	−14.842039	−14.781188	−14.842032	−14.842032
9	−7.543412	−7.375999	−7.543407	−7.543407
10	2.447842	2.593213	2.447833	2.447833
11	8.860350	8.929447	8.860341	8.860341
12	11.367816	11.386463	11.367804	11.367804
IBM 7090 Computer time for 12 hour forecast in minutes		7.2	13.2	19.8

The following discussion is perhaps pertinent here. The experiments have shown that the time and space truncation errors are very small, as explained in the following reasoning. The solutions given by Eq (25), (26), (27) and (28) are linear functions in x and y for all time. The objective analysis scheme (the 9 and the 5 point) is thus capable of getting an exact description of the field for any time, the coefficients of the quadratic term becoming zero exactly. The time truncation is minimized by the many-iterative centered implicit scheme and the many guesses on the exact location of the parcel. As mentioned earlier, this scheme is found to reduce the time truncation considerably. Even though no double precision (for significant figures) was used on the IBM 7090, the high accuracy of the results on Table 4 lies in part in the fact that a non-dimensional-scaling was used to determine the coefficients of the objective analysis scheme.

Other experiments not reported above, showed that the time truncation error did increase when Δt was made larger for the numerical solution of the inertial motions. These errors resulted in a spatial distribution of the velocity field that was not a linear function of x and y and hence space truncation errors developed.

4. Numerical integration of primitive equations

We wish to introduce two simple primitive equation models in this section.

(a) *Mixed gravity-inertia and Rossby waves*

Considerable research on the numerical integration of the primitive equations has begun in the last few years. Some of the major problems associated with this type of numerical work are:

(i) Adjustment of initial data to suppress large amplitude non-meteorological modes;

(ii) Obtaining a stable finite-difference representation of the equations;

(iii) Elimination of non-linear computational modes.

Phillips (1959, 1960) has reviewed these aspects in great detail and the author does not wish to go into them here.

We shall first illustrate a hydrodynamical system capable of propagating both gravity and Rossby waves. The system is an incompressible homogeneous fluid in hydrostatic equilibrium, whose upper surface is free to move and is bounded at the bottom by a rigid horizontal surface.

Eq (1), (2) and (3) would describe this system where

$$P=fv-g\frac{\partial z}{\partial x} \tag{30}$$

$$Q=-fu-g\frac{\partial z}{\partial y} \tag{31}$$

and

$$R=-z\left(\frac{\partial u}{\partial x}+\frac{\partial v}{\partial y}\right). \tag{32}$$

z is the height of the free surface.

We shall introduce the Rossby β-plane approximation and consider an initial distribution given by the following equations:

$$u(x,y,0)=\bar{u}+2\cos\frac{2\pi x}{\lambda}\sin^2\frac{y-y_0}{y_M-y_0}\pi \tag{33}$$

$$v(x,y,0)=\cos\frac{2\pi x}{\lambda}\sin^2\frac{y-y_0}{y_M-y_0}\pi \tag{34}$$

$$z(x,y,0)=\bar{z}(y)+100\cos\frac{2\pi x}{\lambda}\sin^2\frac{y-y_0}{y_M-y_0}\pi. \tag{35}$$

These initial conditions describe a mean zonal flow in geostrophic balance with a mean meridional slope of the free surface, plus a perturbation in the x and y directions whose dimensions are defined by the constants appearing in the equations.

A linear analysis of the x dependent perturbation (only) may be found in Thompson's book (1961). This analysis yields a frequency equation containing three roots for the wave speed. These are, two gravity inertia modes along the $\pm x$ axes and a Rossby wave mode. A linear analysis of the "x, y perturbation" introduced above has not been made but intuitively we should again expect three principal modes.

The following constants are used: $\bar{u}=15$, $\lambda=60°$ longitude. Figs. (2), (3) and (4) show the initial conditions (for u, v and z) schematically with the grid distances $\Delta x=4°$ longitude, $\Delta y=3°$ latitude.

Boundary conditions. The perturbations defined in Eq (33), (34) and (35) have a cyclical continuity in the zonal direction. Along $y=y_0$ and $y=y_M$ the perturbation vanishes. Consistent with this we assume

$$u\left(x, \begin{matrix} y_0 \\ y_M \end{matrix}, t\right)=u\left(x, \begin{matrix} y_0 \\ y_M \end{matrix}, 0\right)=\bar{u} \tag{36}$$

$$v\left(x, \begin{matrix} y_0 \\ y_M \end{matrix}, t\right)=v\left(x, \begin{matrix} y_0 \\ y_M \end{matrix}, 0\right)=0 \tag{37}$$

$$z\left(x, \begin{matrix} y_0 \\ y_M \end{matrix}, t\right)=z\left(x, \begin{matrix} y_0 \\ y_M \end{matrix}, t\right)=\bar{z}\left(\begin{matrix} y_0 \\ y_M \end{matrix}\right). \tag{38}$$

These boundary conditions will confine the growth and propagation of the perturbation between $y_0<y<y_M$ for all time.

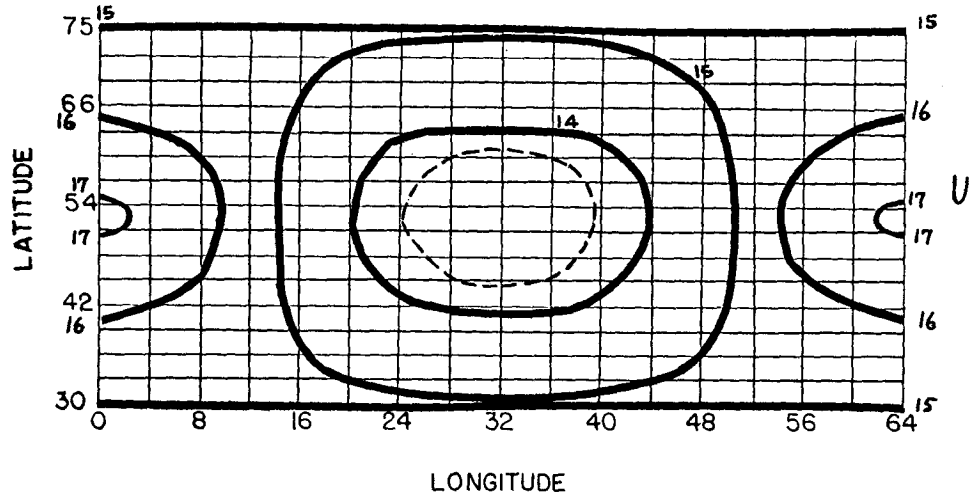

FIG. 2. The initial distribution of the zonal wind, U (m sec^{-1}), obtained from Eq (33) of text.

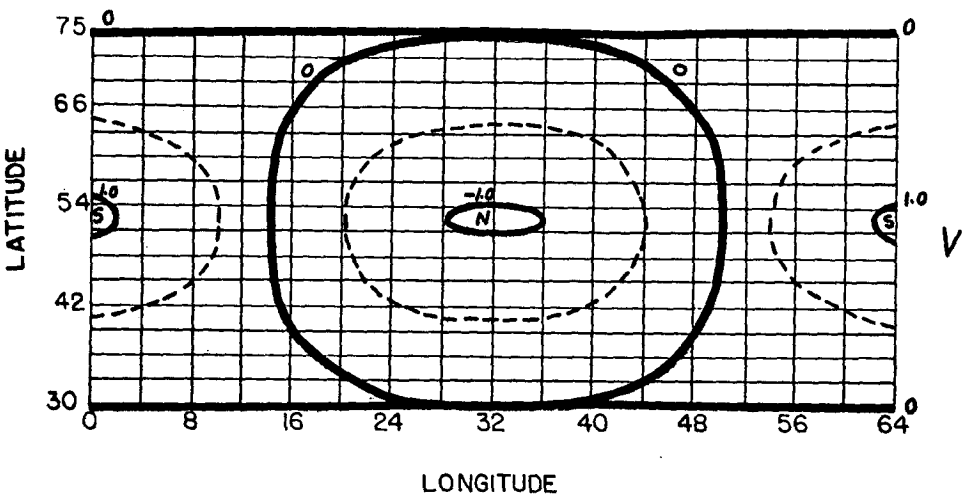

FIG. 3. The initial distribution of the meridional wind, V (m sec^{-1}), obtained from Eq (34) of text.

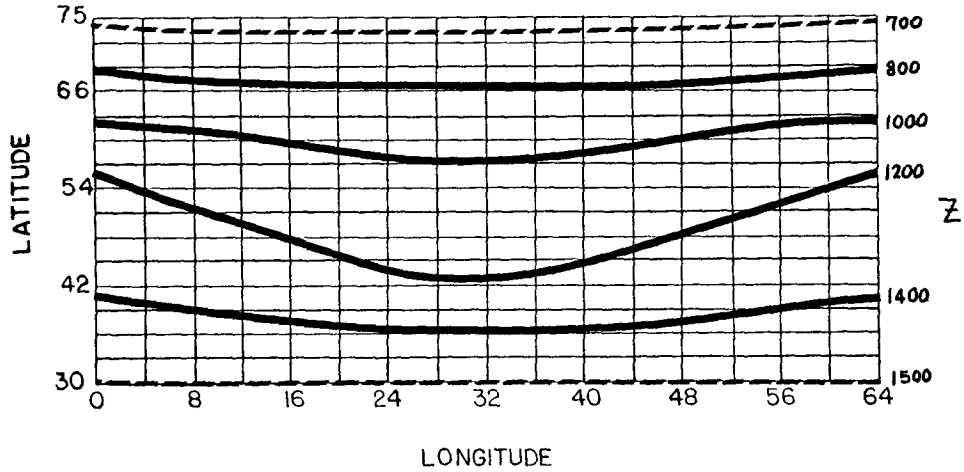

FIG. 4. The initial distribution of the height of the free surface, Z (m), obtained from Eq (35) of text.

Computational stability criterion. The conventional computational stability criteria are obtained by a finite difference representation of the linearized equations. The quasi-Lagrangian representation and the many iterations during a time step make it very difficult to carry out such an analysis.

The expressions for P, Q and R are obtained at each time step by a centered space differencing scheme. For certain choice of time steps the scheme could be expected to be unstable.

In this, and the following example, the computational stability criterion are determined by trial and error on the computer. In part we were guided by the criterion developed by Eliassen[3] for the Eulerian representation of the primitive equations.

$$\frac{\Delta x}{\Delta t} \geq \sqrt{2}\left(\frac{\bar{u}}{2} \pm \sqrt{gz}\right)_{\max} . \tag{39}$$

An important question came up at this stage of the analysis: "For a given ϵ (Eq 21), what determines the most efficient choice of Δt?" Some numerical experiments were carried out to look into this question, and we shall present them in the following section.

A choice of $\epsilon = 10^{-3}$ is made in this experiment, a choice of $\Delta t = 5$ minutes was found to be computationally stable and produced a rapid convergence of the iteration scheme.

The results of the integration for the first 24 hr are shown through a time section along 50N, in Fig. 5. The two wavy lines in the time section are the locations of the cells of maximum and minimum velocity. The rapid oscillations of large amplitude are the gravity-inertia modes that travel with a speed of around 100 msec^{-1}. The dashed lines show a slow eastward propagation of the entire system with a speed very close to that of linear Rossby waves. The experiment was carried out for a period of over 40 hr and the time section appeared very similar.

Perhaps the only other feature in this calculation that may be worth mentioning is the time variation of the meridional profile of the zonal wind, Fig. 2. The initial meridional profile at $x=0$ is a broad wind maximum. Later the north-south profile becomes sharper, perhaps due to the momentum-convergence effect of the non-linear terms. The total kinetic energy of the entire fluid was kept track of throughout the calculations, and it appeared to be unchanged during the first 43 hr.

(b) *Rossby waves—balanced initial conditions*

The so-called Neamtan initial conditions based on work of Haurwitz (1940), Neamtan (1945), have been used for many tests to determine the behavior of

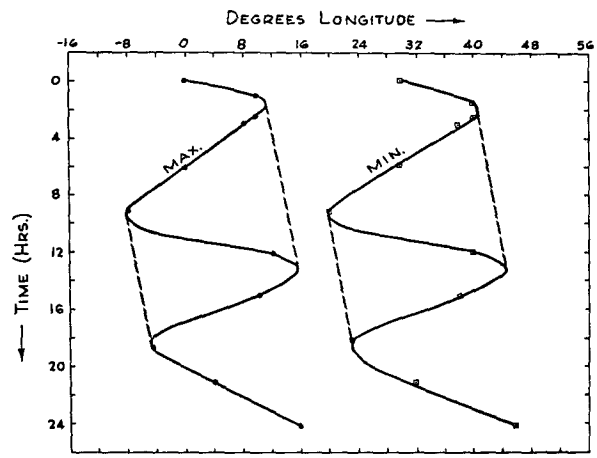

FIG. 5. Time section along 50N latitude showing the position of the wind maximum and minimum whose initial positions are shown in Figs. 2 and 3. The dashed lines indicate the slow eastward propagation of the entire system.

[3] Eliassen, A., 1956: A procedure for numerical integration of the primitive equations of the two-parameter model of the atmosphere. Scientific Report No. 4, on Contract AF 19(604)-1286, Dept. of Meteorology, University of California at Los Angeles, 53 pp.

numerical prediction models. Gates and Riegel (1962) utilized these initial conditions to test their non-divergent barotropic model. Phillips (1959) used a similar set of initial conditions to test the behavior of the primitive equations in a divergent-barotropic atmosphere.

Perhaps the one important advantage of these initial conditions lies in that the streamfunction of the initial wind field satisfies the so-called balance equation. This according to the work of Charney (1955) would result in rather small amplitude gravity-inertia modes. In this section we shall present the initial condition from Phillips (1959). Phillips was concerned with the problem of numerical integration of the primitive equations on the hemisphere and an overlapping Mercator and stereographic grid was utilized. Our aim here is to test the proposed advection scheme for meteorological forecasts and hence we shall take a simple stereographic grid between the equator and 75N, with initial data exactly those of Phillips. The choice of a stereographic grid near the equator will produce a large amplification but perhaps this will not be very critical. The author did not wish to go into a sophisticated hemispheric map projection, like that of Phillips, at this preliminary stage.

The equation of the model may be written as follows:

$$\frac{du}{dt} = -mg\frac{\partial z}{\partial x} + fv \tag{40}$$

$$\frac{dv}{dt} = -mg\frac{\partial z}{\partial y} - fu \tag{41}$$

$$\frac{dz}{dt} = -mz\left(\frac{\partial u}{\partial x} + \frac{\partial v}{\partial y}\right) \tag{42}$$

where m is the scale factor for the stereographic projection

$$m = \frac{2}{(1+\sin\theta)}. \tag{43}$$

The initial conditions are given by the streamfunction

$$\psi(x,y,0) = -a^2\omega \sin\theta + a^2 k \cos^R\theta \sin\theta \cos R\lambda \tag{44}$$

where θ is the latitude, λ the longitude, ω and k are constants with dimensions of angular velocity. R is the hemispheric wave number. The velocity components are given by the equations

$$u(x,y,0) = -\frac{1}{a}\frac{\partial \psi}{\partial \theta}$$

$$v(x,y,0) = \frac{1}{a\cos\theta}\frac{\partial \psi}{\partial \lambda} \tag{45}$$

where the symbol a represents the radius of the earth. The initial height of the free surface is given by the equation

$$z(x,y,0) = z_0 + \frac{a^2}{g}[A(\theta) + B(\theta)\cos R\lambda + c(\theta)\cos 2R\lambda] \tag{46}$$

where

$$A(\theta) = \tfrac{1}{2}\omega(2\Omega+\omega)\cos^2\theta + \tfrac{1}{4}k^2(\cos\theta)^{2R}[(R+1)e^2 + (2R^2-R-2) - 2R^2e^{-2}]$$

$$B(\theta) = \frac{2(\Omega+\omega)k}{(R+1)(R+2)}e^R[(R^2+2R+2) - (R+1)^2e^2]$$

$$c(\theta) = \tfrac{1}{4}k^2e^{2R}[(R+1)e^2 - (R+2)]$$

$$e = \cos\theta.$$

The following values are used for the constants

$$\omega = k = 7.848\times 10^{-6}$$
$$R = 4$$
$$z_0 = 8000.$$

The choice of $z_0 = 8000$ m makes the free surface topography somewhat similar to that of the 300-mb surface in winter. Fig. 6 shows the initial distribution of z. The distributions of u and v are displayed in Figs. 7 and 8. Perhaps to a meteorological eye these initial distributions are mostly acceptable as conditions one would sometimes observe on a chart except perhaps for the large belt of zonal winds near the equator in Fig. 7.

Boundary conditions

The grid used for numerical calculation may be seen in Figs. 6, 7 and 8, where we have taken

$$\Delta x = 6 \text{ deg longitude}$$
$$\Delta y = 5 \text{ deg latitude}.$$

Cyclical continuity in the zonal direction permits four waves around the globe.

As boundary conditions at the equator and at 75N we have permitted the waves at these boundaries to move from west to east without change of shape. This would be consistent with a non-divergent barotropic atmosphere but perhaps not rigorously so (Smagorinsky, 1958) for a divergent primitive equation model. For a closed region the author found these boundary conditions most suitable. The speed of movement of the waves (in u, v and z) at the boundaries were given by the equation for the angular velocity

$$\nu = \frac{R(3+R)\omega - 2\Omega}{(1+R)(2+R)} \tag{47}$$

which is again given by the theory of non-divergent barotropic flow. We have assumed here that the solu-

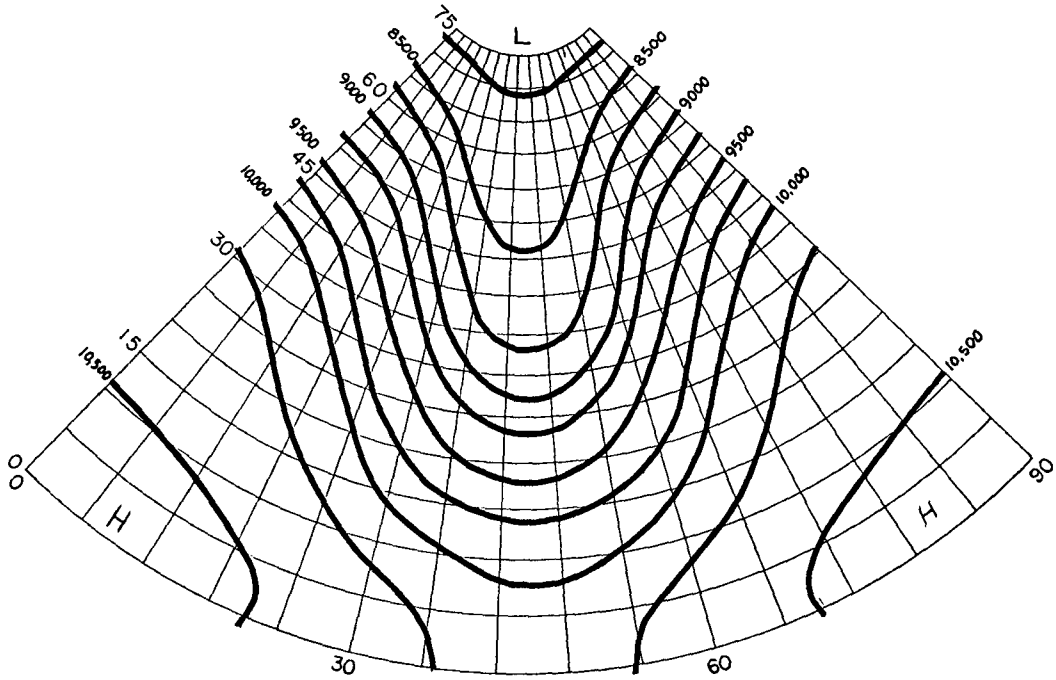

FIG. 6. Initial distribution of Z (m), the height of the face surface, obtained from Eq (46) of text.

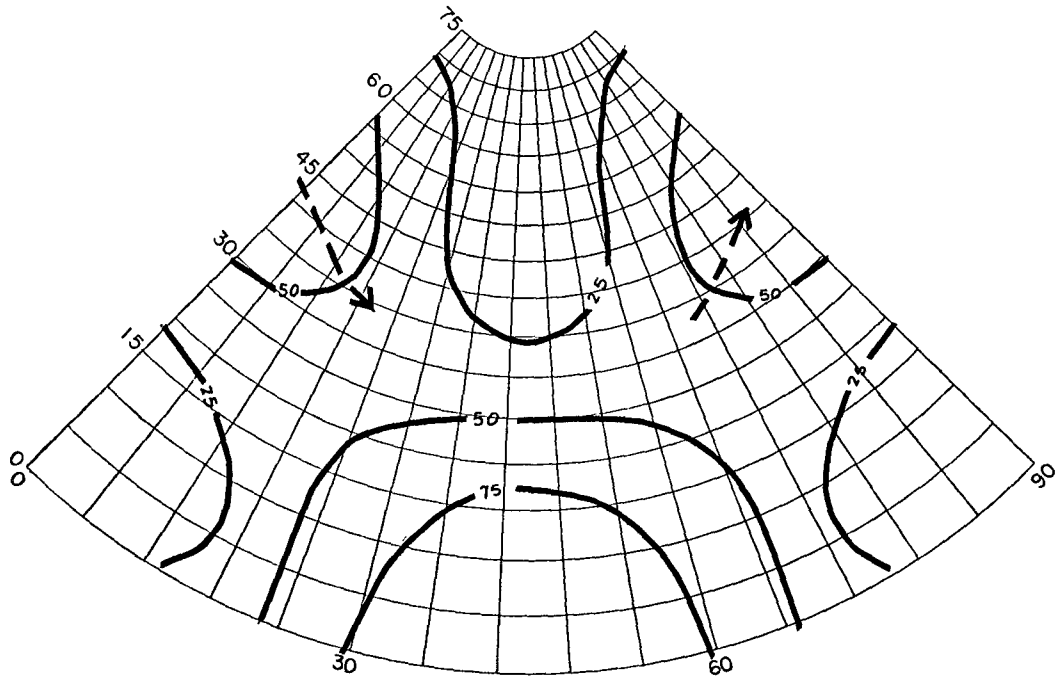

FIG. 7. Initial distribution of U (m sec^{-1}), the zonal wind speed, obtained from Eq (44) and (45) of text.

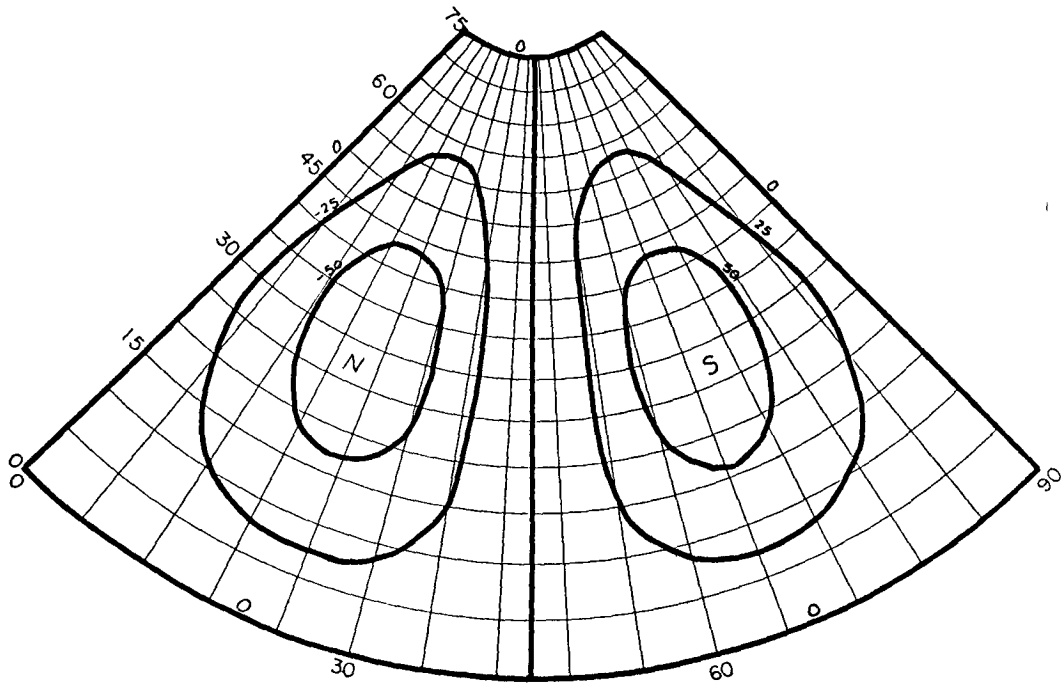

FIG. 8. Initial distribution of V (m sec^{-1}), the meridional wind speed, obtained from Eq (44) and (45) of text.

tion of the divergent primitive equation model would be very close to that of the non-divergent barotropic vorticity equations and hence such a choice of boundary conditions would not complicate the numerical integrations.

Computational stability criterion

As in the previous example, the criterion developed by Eliassen[4] was utilized as a guide in the determination of the computational stability criterion. In this connection Fig. 9 may be worth examining. The abscissa shows the time step, and the ordinate shows the IBM 7090 computer time for 30 time steps. The nine-point quasi-Lagrangian scheme was tested for this example with a choice of $\epsilon = 10^{-3}$. A time step of 15 min was found unstable after a few hours of integration.

The reason for the breakdown of the numerical calculations for $\Delta t \geq 15$ minutes may perhaps be explained by the space-truncation inherent in the 9-point scheme. It is true that an implicit scheme of the type proposed here is known to be stable in a variety of linearized systems; however, once space truncation builds up computations do break down.

In particular one may look at the region near the equator where large wind speeds (≈ 100 m sec^{-1}) are found. The origin of a parcel (point Q of Fig. 1) lies quite far from the forecast point (P in Fig. 1) for $\Delta t \geq 15$ min; in this case larger space truncations are possible.

[4] Same as footnote 3.

Calculations for time steps 4, 8 and 10 min showed that the efficient time step, for the given ϵ, was perhaps between 4 and 8 min. We selected a time step $\Delta t = 5$ min in this problem for a rapid convergence of the proposed advection scheme.

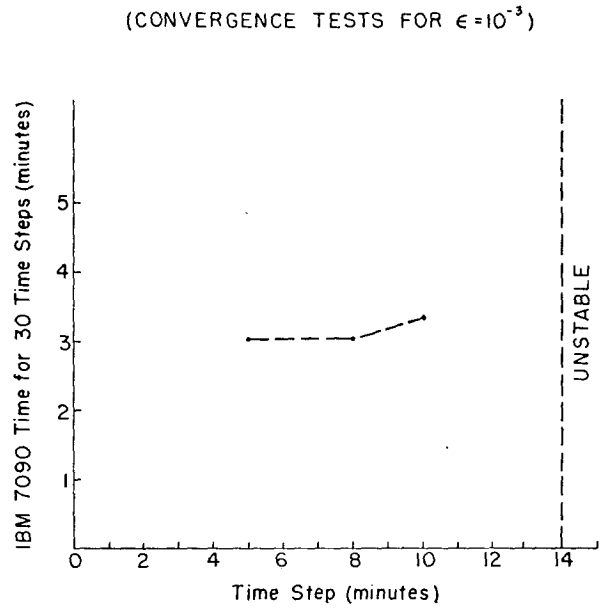

FIG. 9. A graph illustrating the determination of a stable and efficient time step for numerical integration. The abscissa shows the time step and ordinate shows the corresponding IBM 7090 time for 30 iterations. A choice of $\epsilon = 10^{-3}$ is made in these calculations.

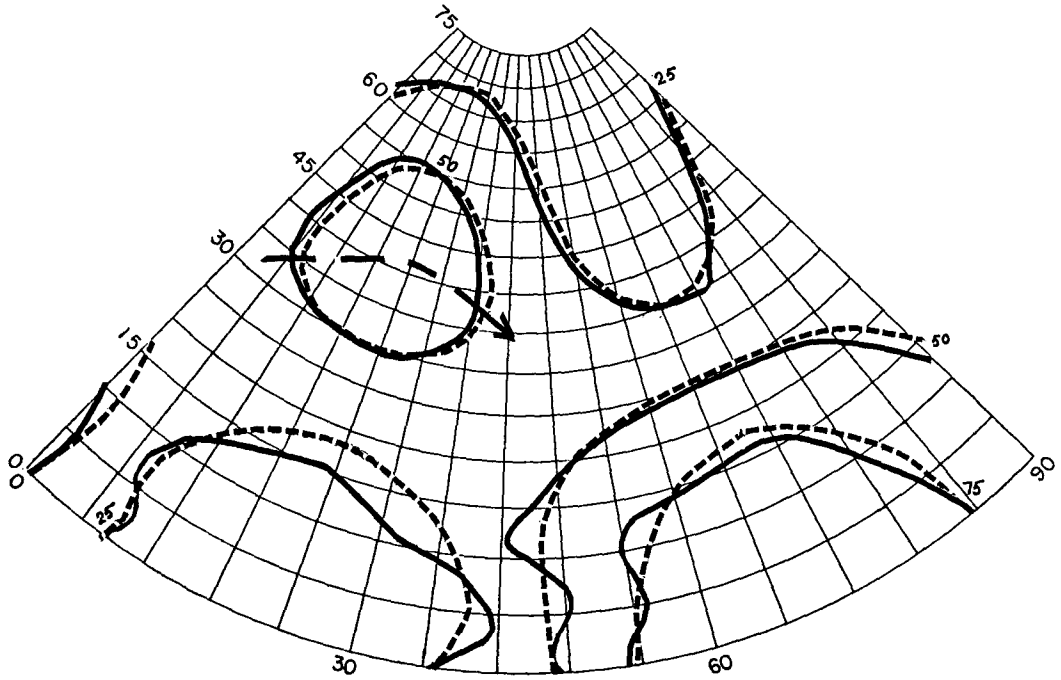

FIG. 10. Forty-eight hour numerical forecast field of the zonal wind speed, U (m sec^{-1}), shown by continuous lines. The dashed lines indicate the corresponding solution for barotropic non-divergent flow.

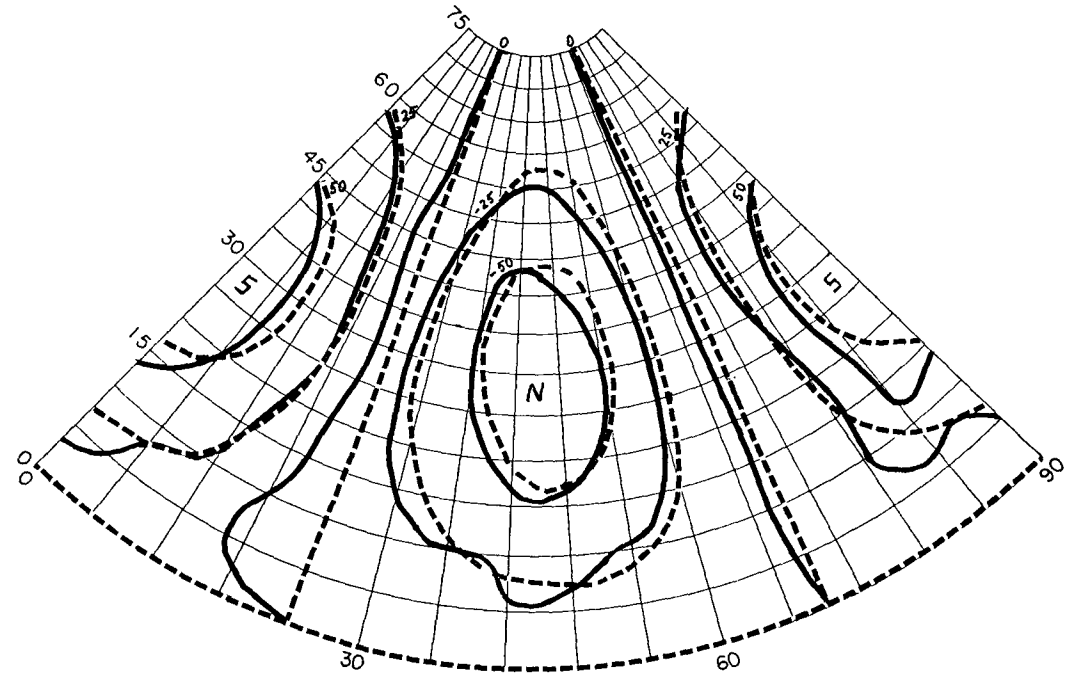

FIG. 11. Forty-eight hour numerical forecast field of the meridional wind speed (m sec^{-1}) shown by continuous lines. The dashed lines indicate the corresponding solution for barotropic non-divergent flow.

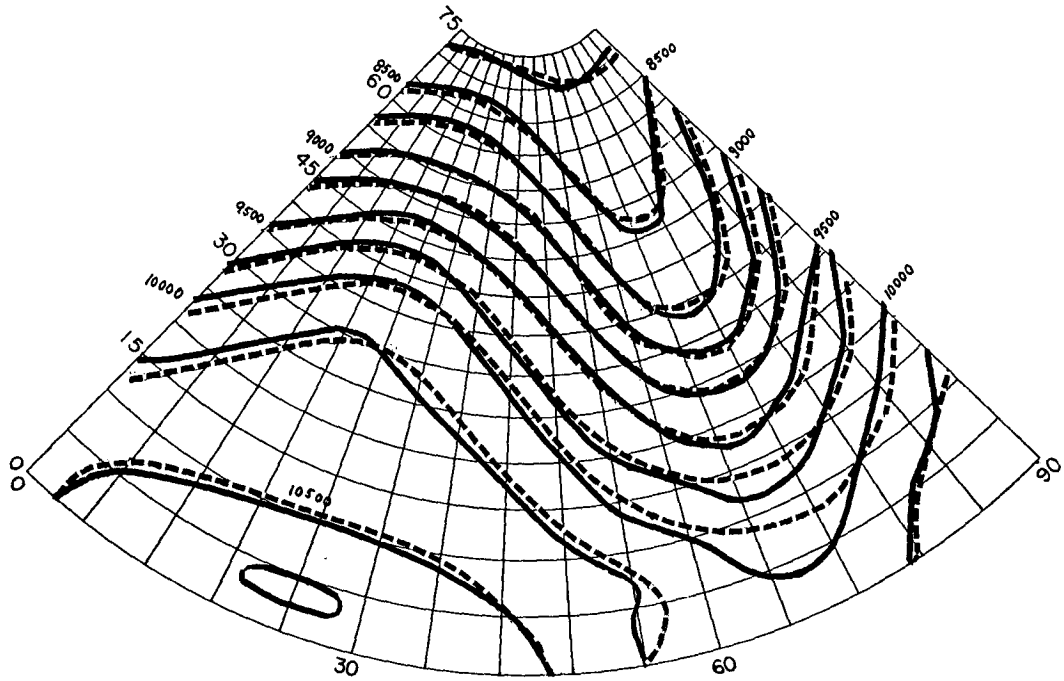

FIG. 12. Forty-eight hours numerical forecast field of the height of the free surface Z (m), shown by continuous lines. The dashed lines indicate the corresponding solution for barotropic non-divergent flow.

The results of the computations. The numerical calculations were carried out for a period of 48 hr. By this time a small disturbance had originated at a lower latitude between the equator and 15N. Though this feature was already noticed at the 12-hr forecast it did not appear to amplify. The author believes that in part the reason for this lies in the choice of a stereographic projection all the way to the equator. Perhaps our choice of the boundary condition for the divergent atmosphere from the non-divergent barotropic flow produces the irregularities. Figs. 10, 11 and 12 (continuous lines) display the forecast field of u, v and z at 48 hr. The dashed lines show the corresponding solutions for the barotropic non-divergent flow. In middle and higher latitudes the solution of the primitive equation model appears to be very close to the motion without change of shape. The movements of the waves are a little slower than for the non-divergent barotropic atmosphere.

The total mean square kinetic energy and relative vorticity of the flow over the entire area were evaluated after every 2 hr and the results did not appear to alter significantly in 48 hr.

The experiment was stopped after 48 hr of integration because of the difficulties encountered at the lower latitudes.

5. Some concluding remarks

The calculation presented above suggests that the quasi-Lagrangian integration scheme may be an efficient scheme for numerical integration of meteorological equations. The model with simple initial conditions given by Eq (22) and (23) yields solutions that are linear functions of x and y for all time. This definitely limits the scope of these tests. The two primitive equation models contain simple wave patterns as initial conditions, and a good test on the non-linear behavior of a model should perhaps permit interaction between many wave numbers.

The limitations mentioned above are unavoidable at a preliminary stage of testing. The author wishes to look into the behavior of a model that is known to exhibit non-linear computational instability for a finite-difference Eulerian representation. Perhaps a test on such a model might be rewarding in establishing the usefulness of the model.

Acknowledgments. The author has benefited a great deal from discussions with Professors M. G. Wurtele, W. L. Gates and Dr. A. Arakawa.

The computations were performed on the IBM 7090, and appreciation is expressed to the Numerical Analysis Center of the University of California for making the computer time available for this work.

The research reported in this paper was in part sponsored by the Office of Naval Research, Contract No. Nonr-233(21).

APPENDIX

Consider the system of equations:

$$\frac{du}{dt}=\frac{\partial u}{\partial t}+u\frac{\partial u}{\partial x}+v\frac{\partial u}{\partial y}=0 \tag{A1}$$

$$\frac{dv}{dt}=\frac{\partial v}{\partial t}+u\frac{\partial v}{\partial x}+v\frac{\partial v}{\partial y}=0. \tag{A2}$$

Subject to the initial conditions:

$$\begin{aligned} u(x,y,0)&=Ax+By \\ v(x,y,0)&=Cx-Ay \end{aligned} \tag{A3}$$

where A, B and C are constants. Eq (1) and (2) may be solved analytically for the initial condition (3) by the following procedure.

In a time interval t a parcel now at x, y and originally at x', y' has travelled the distances

$$x-x'=(Ax'+By')t \tag{A4}$$

$$y-y'=(Cx'-Ay')t. \tag{A5}$$

The pair of transcendental Eq (4) and (5) may be solved for x', y' in terms of x, y and t.

$$x'=\frac{\begin{vmatrix} x & Bt \\ y & 1-At \end{vmatrix}}{\begin{vmatrix} 1+At & Bt \\ Ct & 1-At \end{vmatrix}}$$

$$y'=\frac{\begin{vmatrix} 1+At & x \\ Ct & y \end{vmatrix}}{\begin{vmatrix} 1+At & Bt \\ Ct & 1-At \end{vmatrix}}.$$

Since $du/dt=dv/dt=0$ for this case, therefore

$$\begin{aligned} u(x,y,t)&=u(x',y',0) \\ v(x,y,t)&=v(x',y',0) \end{aligned}$$

or

$$\begin{aligned} u(x,y,t)&=Ax'+By' \\ v(x,y,t)&=Cx'-Ay' \end{aligned}$$

and we obtain,

$$u(x,y,t)=\frac{A[(1-At)x-Bty]+B[(1+At)y-Ctx]}{1-(A^2+B)Ct^2} \tag{A6}$$

$$v(x,y,t)=\frac{c[(1-At)x-Bty]-A[(1+At)y-Ctx]}{1-(A^2+BC)t^2}. \tag{A7}$$

REFERENCES

Charney, J., 1952: The use of the primitive equations of motion in numerical prediction. *Tellus*, **7**, 22–26.

Fjørtoft, R., 1952: On a numerical method of integrating the barotropic vorticity equation. *Tellus*, **4**, 179–194.

——, 1955: On the use of space-smoothing in physical weather forecasting. *Tellus*, **7**, 179–194.

Gates, W. L., and C. A. Riegel, 1962: A study of numerical errors in the integration of barotropic flow on a spherical grid. *J. geophys. Res.*, **67**, 773–784.

Haurwitz, B., 1940: The motion of atmospheric disturbances on the spherical earth. *J. marine Res.*, **3**, 254–267.

Levy, H., and E. A. Baggott, 1950: *Numerical solution of differential equations*. New York, Dover Publication, Inc., 238 pp.

Neamtan, S. M., 1946: The motion of harmonic waves in the atmosphere. *J. Meteor.*, **3**, 53–56.

Økland, H., 1962: An experiment in numerical integration of the barotropic equation by a quasi-Lagrangian method. *Geofysiske Publikasjoner*, **22**, 1–10.

Phillips, N. A., 1959: Numerical integration of primitive equations on the hemisphere. *Mon. Wea. Rev.*, **87**, 333–345.

——, 1960: On the problem of initial data for the primitive equations. *Tellus*, **12**, 121–126.

Smagorinsky, J., 1958: On the numerical integration of the primitive equations of motion for baroclinic flow in a closed region. *Mon. Wea. Rev.*, **86**, 457–466.

Thompson, P. D., 1961: *Numerical weather analysis and prediction*. New York, The Macmillan Company, 170 pp.

Van-Mieghem, J. M., 1951: Hydrodynamical instability. *Compendium of meteorology*. Boston, American Meteorological Society, 434–453.

Wiin-Nielsen, A., 1959: On the application of trajectory methods in numerical forcasting. *Tellus*, **11**, 180–196.